UNITED STATES DEPARTMENT OF THE INTERIOR

U. S. GEOLOGICAL SURVEY

BULK AND SHEAR MODULI OF NEAR-SURFACE GEOLOGIC UNITS NEAR THE SAN ANDREAS FAULT AT PARKFIELD, CALIFORNIA

M. Stewart and M. J. S. Johnston

Open-File Report 93-378

1993

ABSTRACT

*Shear and bulk moduli have been measured as a function of depth in three boreholes along a 50 kilometer section of the San Andreas fault near Parkfield, California. The shear modulus values range from 1.45 * 10^7 to 8.69 * 10^8 pascals at depths as great as 180 meters, and show a general increase with depth. The values of bulk modulus also increase with depth and range from 8.27 * 10^7 to 4.48 * 10^9 pascals to depths of 180 meters. These values are significantly lower than moduli values reported for unfractured crystalline rocks. Low rigidity and bulk modulus in fault zone materials could account for many of the apparent physical properties and behavior of this section of the San Andreas fault. These properties include low earthquake stress drops, low heat flow, "blocklike" fault slip behavior, and would suggest that strainfields and strain energy release are concentrated near the fault. Similar measurements at other borehole locations along the fault and at points off the fault are needed to fully quantify these effects.*

INTRODUCTION

In 1985 the U.S.Geological Survey initiated an experiment to attempt to predict the next moderate magnitude earthquake on the San Andreas fault near Parkfield California (Bakun and Lindh, 1985). The Parkfield section of the San Andreas fault has a history of moderate-size magnitude 6 earthquakes that repeat, on average, about every 21 to 22 years. The most recent event occurred on June 28, 1966 and ruptured a 20-30 km section of the fault from Middle Mountain to Cholame. The Parkfield section of the San Andreas fault is a transition zone between an aseismic "creeping" section to the northwest and the "locked" Cholame section to the southeast. The Creeping section experiences frequent small earthquakes (< M4), while the Cholame section frequently has large earthquakes of magnitude greater than six. By intensively monitoring the area with various types of geophysical instruments, seismologists hope to provide advanced warning of the next serious earthquake.

One of the monitoring techniques used concerns continuous measurement of the state of crustal strain using dilational and tensor strainmeters with sensitivity of less than 10^{-10}. These instruments are cemented into the bottom of deep boreholes along the fault and at distances of a few kilometers from the fault where the strains from deep fault slip are expected to be a maximum (Johnston et al., 1987). Ten strainmeters have been installed in the Parkfield region (Myren and Johnston, 1989). Prior to the installation of eight of these strainmeters in 1986, seismic wave velocities were measured in a number of the open boreholes to establish the depth dependence of seismic parameters in the near-surface geologic units (Gibbs and Roth, 1989; Gibbs et al, 1990). It is the intent of this paper to enhance the interpretation of ground displacement, velocity,

acceleration, tilt and strain measurements in the near-surface geologic units by providing direct measurements of bulk and shear moduli as a function of depth in these same boreholes.

Borehole Description

In this report moduli for three boreholes are calculated from Gibbs' velocity data. The boreholes used in this study are located along the fault from northwest to southeast at sites known as Stockdale Mountain, Vineyard Canyon, and Red Hills. A map of the area showing the borehole locations from Gibbs et al., (1990) is shown in Figure 1. The near-surface geologic units alternate between claystones, siltstones, sandstones, and gravels. A complete discussion of the complex geology of the Parkfield area can be found in Sims (1988, 1989).

Stockdale Mountain, the most northern hole, is located to the west of the fault at 35° 58.4' North and 120° 34.6' West. Velocity data from Stockdale Mountain reaches a depth of 155 meters, all of which is in the Upper Miocene Santa Margarita Formation (Tsm). The first 30 meters of Tsm is siltstone which grades into sandstone reaching a depth of 105 meters. The formation then becomes clay at 105 meters and sandstone again at 175 meters.

The Vineyard Canyon site is located west of the fault at 35° 55.3' North and 120° 32.0' West. Velocity data from Vineyard Canyon reaches a depth of 195 meters, unfortunately drill cuttings used in calculating density only reach a depth of 162 meters. The drill cuttings are entirely within the Pleistocene and Pliocene Paso Robles Formation (QTp). At this location the QTp is cross-stratified, lenticular bedded, sands and gravels.

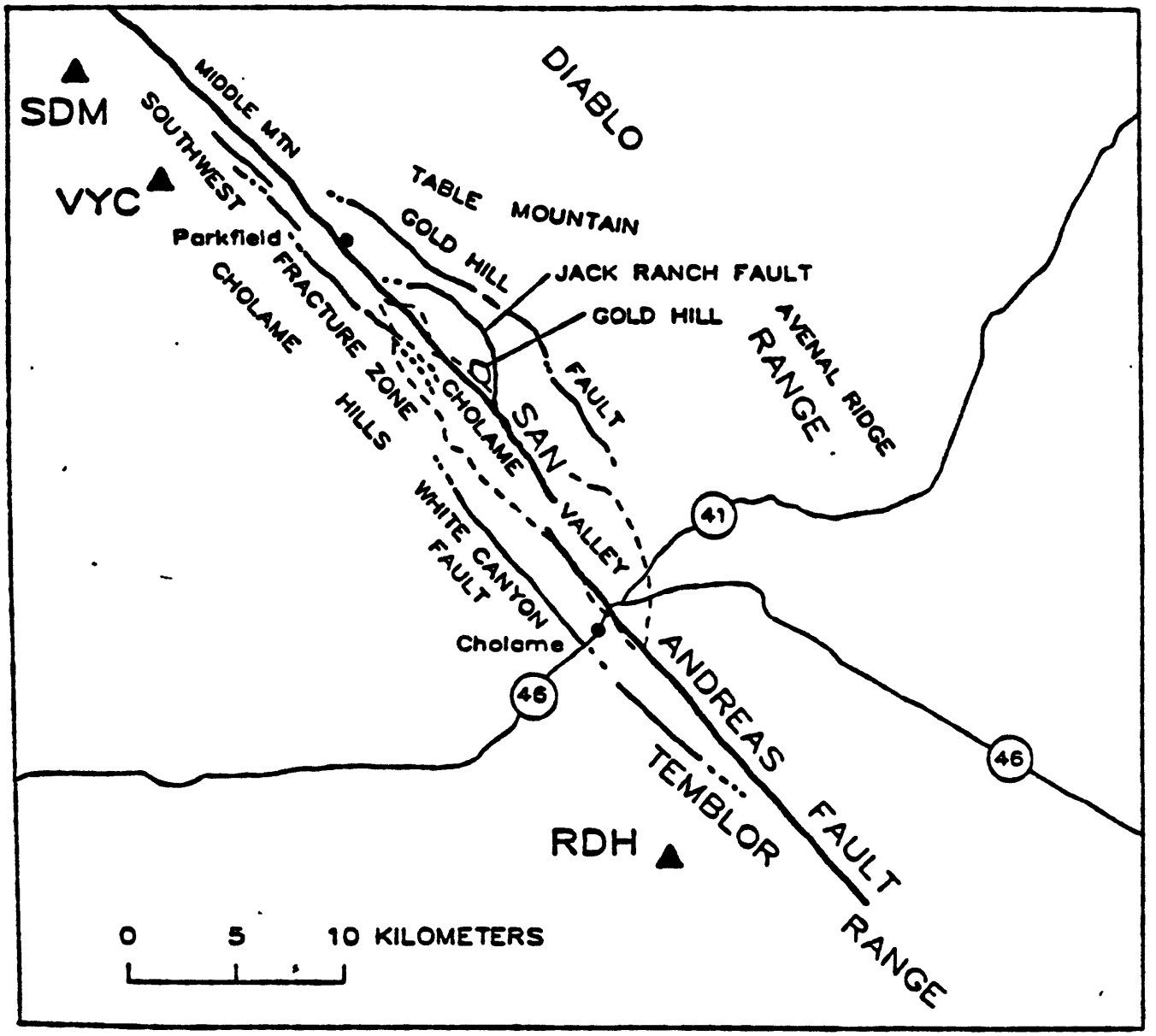

Figure 1

Borehole sites along the San Andreas fault near Parkfield (after Gibbs et al., 1989)

The Red Hills site is located west of the San Andreas fault at 35° 37.5' North and 120° 15.3' West. Velocity data for this hole reaches a depth of 180 meters. The first 175 meters are in the Pleistocene Paso Robles Formation (QTp), alternating clays and sandstones. The final 5 meters of data are in the middle Tertiary Caliente Formation, a claystone at this depth.

Procedure

Provided that density (ρ), shear wave velocity (V_s), and compressional velocity (V_p) are measured with sufficient accuracy, the bulk (K) and shear moduli (μ) for the near-surface units can be calculated from the equations;

$$V_p = \sqrt{\frac{K+4/3\mu}{\rho}} \tag{1a}$$

$$V_s = \sqrt{\frac{\mu}{\rho}} \tag{1b}$$

respectively (Stacey, 1969). For the boreholes investigated, P-wave and S-wave velocities were obtained from Gibbs fIet alfR (1990). These velocities were calculated from Time-Depth graphs and are reported in 2.5 meter increments. Densities were obtained from drill cuttings collected in 20 foot intervals using the procedure described below.

To calculate the densities from drill cuttings, the cuttings first had to be crushed to grain size. They were then pressed into a cell of known mass and volume. These cells were then placed in a vacuum chamber and were saturated with distilled water. The mass of the saturated sample was measured on an analytical balance. The density was calculated from this measurement as follows.

TOTAL MASS - CELL MASS = (SAMPLE MASS)/(CELL VOLUME) = DENSITY

Results

Observations of V_p, V_s, density (ρ), shear modulus (μ), bulk modulus (K), as a function of depth for each of the boreholes are listed in Tables 1a, 1b, and 1c. Plots of μ , K, and ρ as a function of depth are shown in Figures 2a, 2b, 2c, Figures 3a, 3b, 3c, and 4a, 4b, 4c respectively.

DISCUSSION

The results of the density calculations, when plotted with depth in Figures 4a, 4b, and 4c, show little correlation between ρ and depth. The values of density for the three boreholes range from $1.65 * 10^3$ Kg/m^3 to $2.33 * 10^3$ Kg/m^3. Density primarily varies as a function of lithology at such shallow depths and the absence of a correlation between depth and density was expected.

Conversely, the values of μ and K do increase with depth as anticipated. Values of μ for the three boreholes are initially as low as $1.45 * 10^7$ pascals and increase to as much as $8.69 * 10^8$ pascals. Similarly, K increases from $8.27 * 10^7$ pascals to $4.48 * 10^9$ pascals. The apparent conclusion from these results is that at these shallow depths the values of the moduli are primarily dependent on the seismic wave velocities, and that density has little effect on the bulk (K) and shear (μ) moduli.

The values of μ and K obtained for these near-fault sites are clearly lower than those expected and reported for competent basement rocks (Birch, 1966). A critical issue concerns whether these low values generally occur along the fault and are indicative of those expected for a weak fault system. In such a system most of the fault displacement would occur in the fault zone materials and relatively little deformation would occur in the materials at some distance from the fault. The general behavior of

Table 1a - Stockdale Mountain

Depth m	S Velocity m/s	P Velocity m/s	Density 10^3 Kg/m^3	Shear Modulus 10^8 Pa	Bulk Modulus 10^8 Pa
2.5	107	284	1.265	.1448	.8272
5.0	143	364	1.265	.2587	1.331
7.5	178	436	1.349	.4274	1.995
10.0	225	552	1.349	.6829	3.200
12.5	254	586	1.727	1.114	4.445
15.0	284	636	1.727	1.393	5.128
17.5	302	710	1.727	1.575	6.606
20.0	332	747	2.074	2.286	8.525
22.5	355	808	2.074	2.614	10.06
25.0	366	838	1.984	2.658	10.39
27.5	380	891	1.984	2.865	11.93
30.0	406	940	1.984	3.270	13.17
35.0	420	950	1.984	3.500	13.24
40.0	438	1031	2.004	3.845	16.18
45.0	446	1006	2.018	4.014	15.08
50.0	476	1072	2.144	4.858	18.16
55.0	483	974	2.174	5.072	13.86
60.0	493	1028	2.174	5.284	15.93
65.0	514	1011	2.247	5.936	15.05
70.0	533	1058	2.087	5.929	15.46
75.0	546	1055	2.056	6.129	14.71
80.0	555	1109	2.091	6.441	17.13
85.0	566	1133	2.091	6.699	17.91
90.0	578	1155	2.229	7.447	19.81
95.0	591	1189	2.103	7.345	19.94
100.0	597	1207	2.356	8.397	23.13
105.0	616	1239	2.102	7.976	21.63
110.0	614	1268	2.287	8.622	25.27
115.0	615	1283	2.287	8.650	26.11
120.0	619	1309	2.267	8.686	27.26
125.0	629	1322	1.909	7.553	23.29
130.0	638	1334	1.849	7.526	22.87
135.0	630	1345	2.016	8.002	25.80
140.0	630	1368	2.016	8.002	27.06
145.0	644	1391	1.925	7.984	26.60
150.0	660	1412	1.854	8.076	26.20
155.0	671	1445	1.662	7.483	24.73

Table 1.

Values of V_p, V_s, density (ρ), shear modulus (μ), and bulk modulus (K), as a function of depth for the boreholes at; a) Stockdale Mountain, b) Vineyard Canyon, and c) Red Hills.

Table 1b - Vineyard Canyon

Depth m	S Velocity m/s	P Velocity m/s	Density 10^3 Kg/m^3	Shear Modulus 10^8 Pa	Bulk Modulus 10^8 Pa
2.5	____	325	1.653	_____	_____
5.0	____	538	1.867	_____	_____
7.5	____	750	1.821	_____	_____
10.0	____	971	1.539	_____	_____
12.5	245	1096	1.539	.9238	17.25
15.0	249	746	1.723	1.068	8.165
17.5	256	758	1.731	1.134	8.434
20.0	265	826	2.039	1.432	1.200
22.5	272	830	2.039	1.509	1.203
25.0	282	806	2.137	1.699	1.162
*27.5	282	811	1.874	1.490	1.034
*30.0	296	794	1.874	1.642	9.625
32.5	308	835	2.293	2.175	13.09
35.0	311	799	2.293	2.218	11.68
*37.5	320	803	1.991	2.039	10.12
40.0	330	823	2.179	2.373	11.59
42.5	322	840	2.097	2.174	11.90
45.0	333	841	2.231	2.474	12.48
47.5	340	841	2.285	2.641	12.64
50.0	341	856	2.285	2.657	13.20
52.5	350	884	2.200	2.695	13.60
55.0	385	911	2.223	2.849	18.45
57.5	358	952	____	____	____
60.0	365	979	2.069	2.756	16.16
62.5	367	1003	2.168	2.920	17.92
65.0	375	1011	2.168	3.049	18.09
67.5	379	1020	2.023	2.906	17.17
70.0	383	1042	2.175	3.190	19.36
72.5	396	1049	2.059	3.229	18.35
75.0	397	1055	2.095	3.302	18.92
77.5	402	1060	2.095	3.386	19.02
80.0	409	1080	2.017	3.374	19.03
82.5	421	1071	2.006	3.555	18.27
85.0	420	1051	2.036	3.592	17.70
87.5	422	1044	2.059	3.667	17.55
90.0	428	1086	2.104	3.854	19.68
92.5	444	1091	2.104	4.148	19.51
95.0	437	1059	2.017	3.852	17.48
97.5	443	1063	2.110	4.141	18.32

(Continued)

Table 1c - Vineyard Canyon (Continued)

Depth m	S Velocity m/s	P Velocity m/s	Density 10^3 Kg/m^3	Shear Modulus 10^8 Pa	Bulk Modulus 10^8 Pa
100.0	448	1080	2.027	4.068	18.22
102.5	454	1107	2.027	4.178	19.27
105.0	459	1122	2.027	4.271	19.82
107.5	458	1114	2.013	4.223	19.35
110.0	465	1128	2.013	4.353	19.81
112.5	473	1154	2.055	4.598	21.24
115.0	470	1156	2.055	4.539	21.41
117.5	480	1147	2.055	4.735	20.72
120.0	477	1151	———	———	———
122.5	482	1152	2.104	4.888	21.40
125.0	489	1124	2.047	4.895	19.33
127.5	484	1188	2.047	4.795	22.50
130.0	485	1129	2.047	4.815	19.67
132.5	498	1142	2.060	5.109	20.05
135.0	493	———	2.140	5.202	———
137.5	497	———	2.140	5.286	———
140.0	501	1177	2.140	5.371	22.48
142.5	511	———	2.092	5.463	———
145.0	513	1229	2.092	5.505	24.26
147.5	516	1210	2.092	5.570	23.20
150.0	508	1221	2.092	5.399	23.99
152.5	520	1212	2.060	5.570	22.83
155.0	526	1214	2.060	5.700	22.76
157.5	———	1224	2.018	———	———
160.0	———	1216	2.018	———	———
162.5	543	1207	2.018	5.950	21.47

Table 1c - Red Hills

Depth m	S Velocity m/s	P Velocity m/s	Density 10^3 Kg/m^3	Shear Modulus 10^8 Pa	Bulk Modulus 10^8 Pa
2.5	151	347	1.823	.4157	1.641
5.0	199	471	1.823	.7219	3.082
7.5	230	545	1.746	.9236	3.955
10.0	251	649	1.746	1.100	5.818
12.5	280	586	1.921	1.506	4.589
15.0	318	636	1.921	1.943	5.180
17.5	329	658	2.243	2.428	6.474
20.0	317	675	2.243	2.254	7.214
25.0	313	666	2.289	2.243	7.162
30.0	334	689	2.233	2.491	7.279
35.0	368	709	2.233	3.024	7.193
40.0	389	736	2.371	3.588	8.060
45.0	414	747	2.260	3.874	7.446
50.0	418	817	2.300	4.019	9.994
55.0	432	844	2.235	4.171	10.36
60.0	440	894	2.235	4.327	12.09
65.0	454	928	2.449	5.048	14.36
70.0	464	971	2.280	4.909	14.95
75.0	478	1000	2.303	5.262	16.01
80.0	483	1027	2.232	5.201	16.61
85.0	499	1052	2.232	5.558	17.29
90.0	510	1100	2.306	5.998	19.91
95.0	511	1135	2.226	5.813	20.93
100.0	521	1153	2.221	6.029	21.49
105.0	516	1185	2.134	5.682	22.39
110.0	538	1214	2.299	6.654	25.01
115.0	539	1243	2.299	6.679	26.62
120.0	___	1256	2.298	___	___
125.0	522	1257	2.319	6.319	28.22
130.0	521	1270	2.242	6.086	28.05
135.0	523	1319	2.320	6.346	31.90
140.0	515	1318	2.320	6.153	32.10
145.0	520	1328	2.261	6.114	31.72
150.0	522	1339	2.371	6.461	33.90
155.0	511	1371	2.240	5.849	34.31
160.0	511	1390	2.317	6.050	44.77
165.0	522	1411	2.201	5.997	35.82
170.0	522	1411	2.333	6.357	37.97
175.0	536	1424	2.333	6.703	38.37
180.0	542	1443	2.171	6.378	36.70

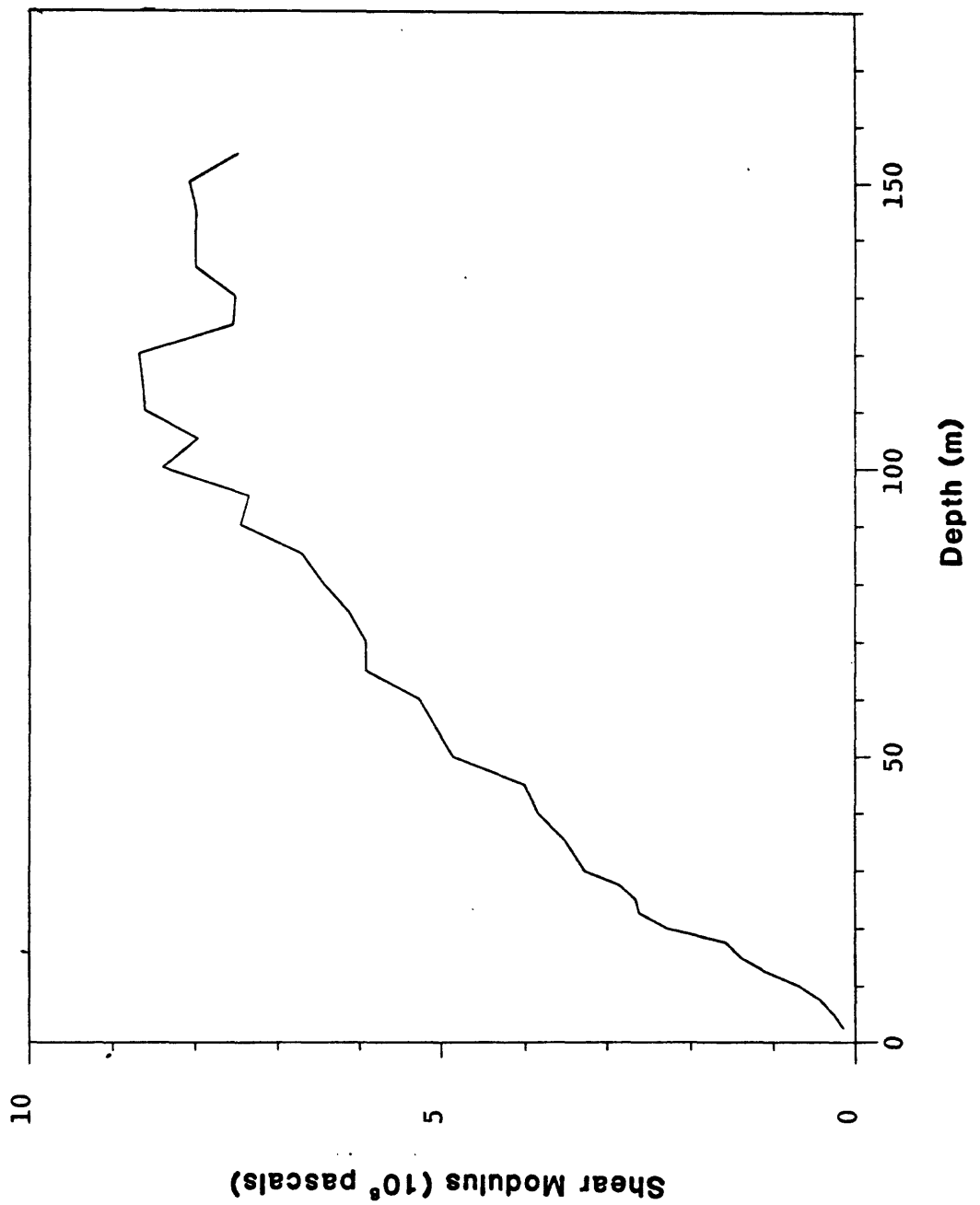

Figure 2a

Plot of μ (10^8 Pa.) as a function of depth (meters) for the Stockdale Mountain site.

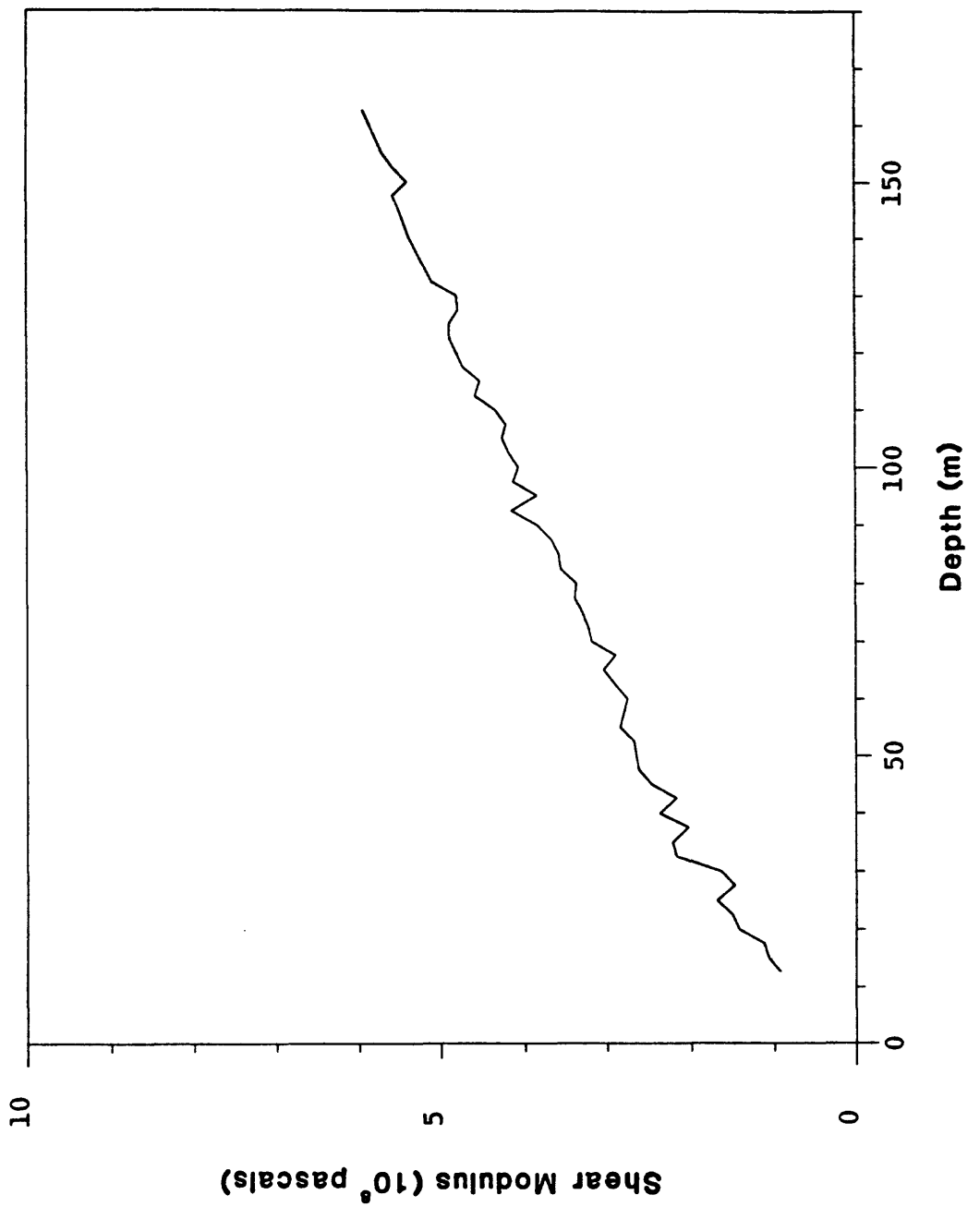

Figure 2b

Plot of μ (10^8 Pa.) as a function of depth (meters) for the Vineyard Canyon site.

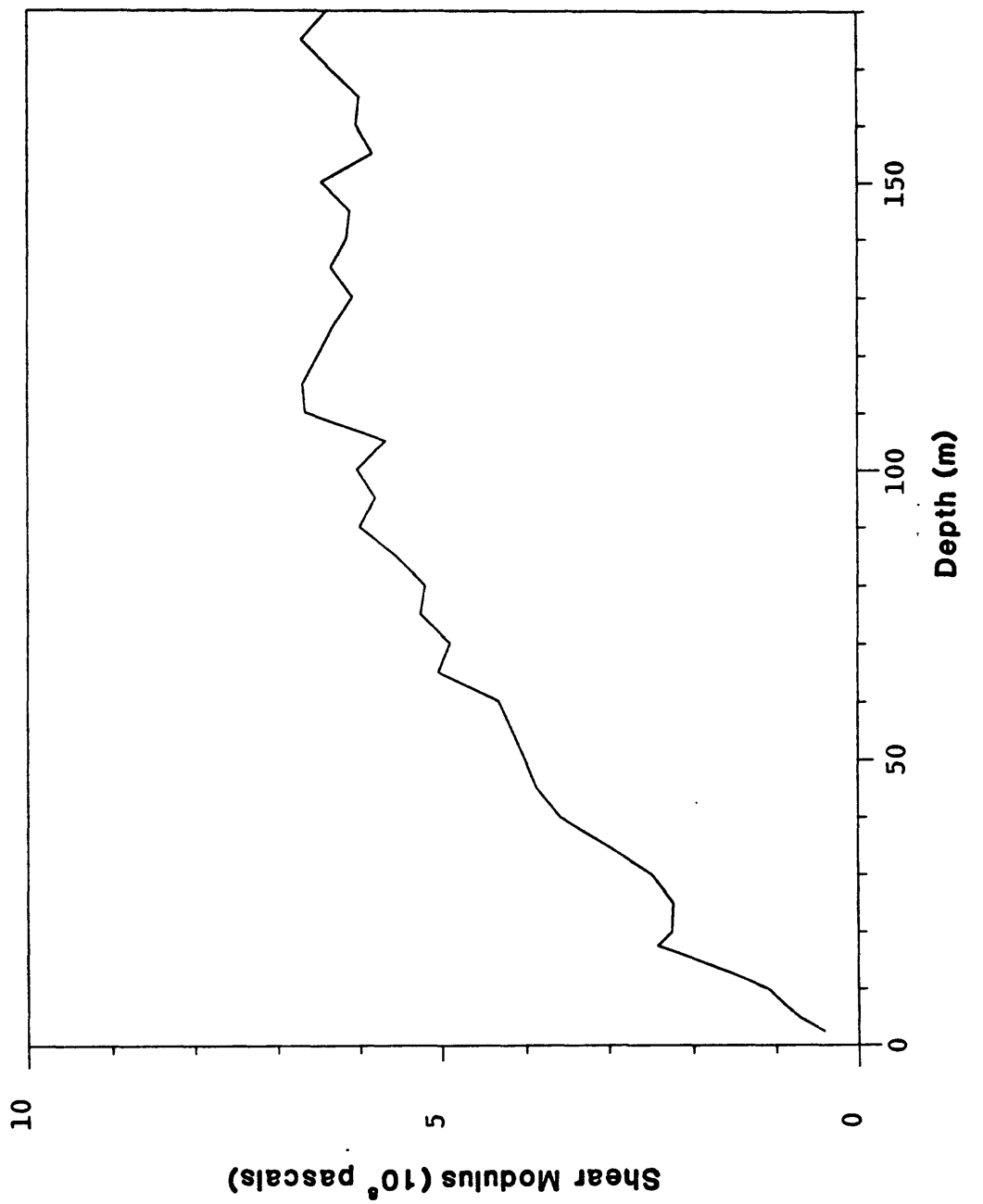

Figure 2c

Plot of μ (10^9 Pa.) as a function of depth (meters) for the Red Hills site.

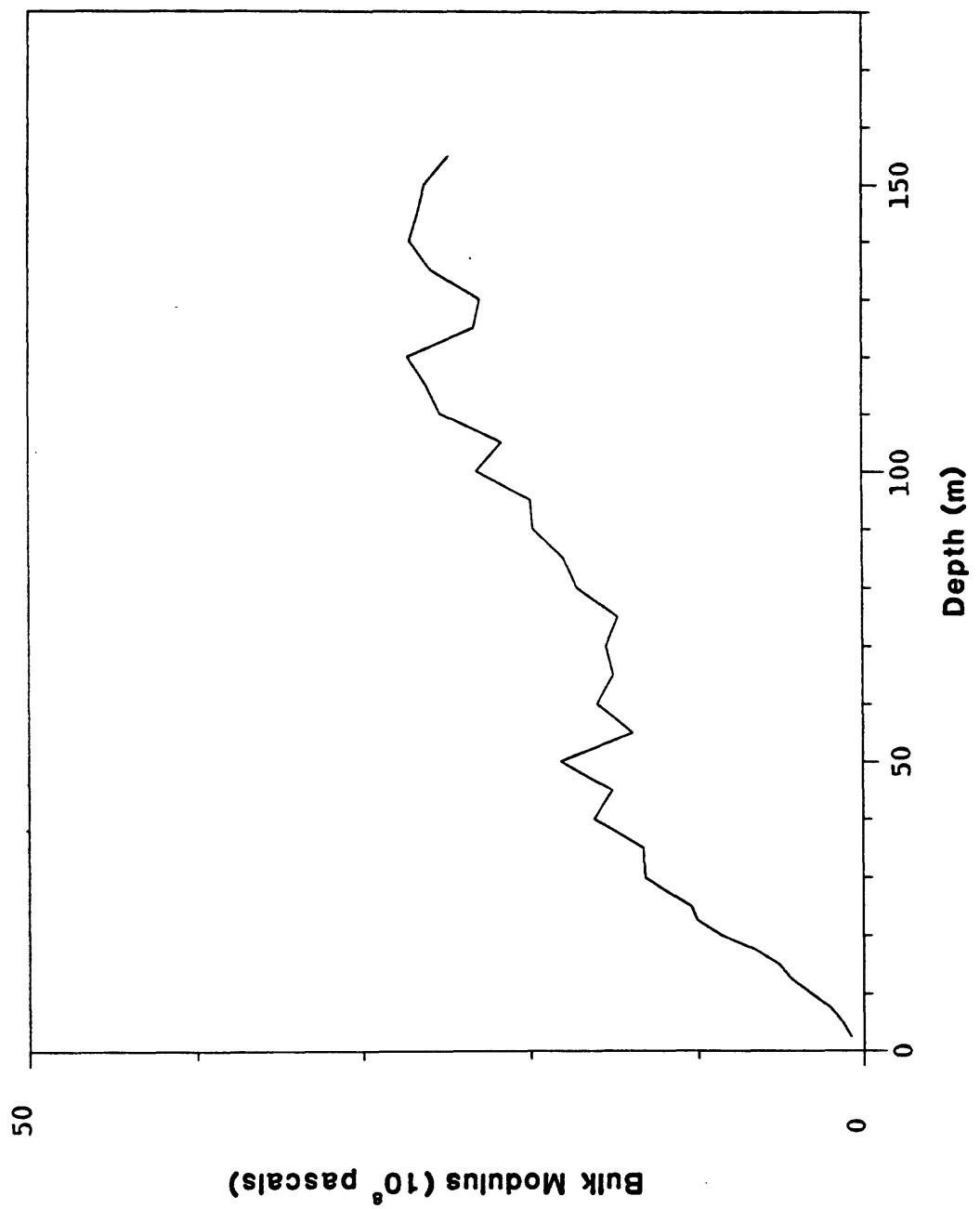

Figure 3a

Plot of K (10^8 Pa.) as a function of depth (meters) for the Stockdale Mountain site.

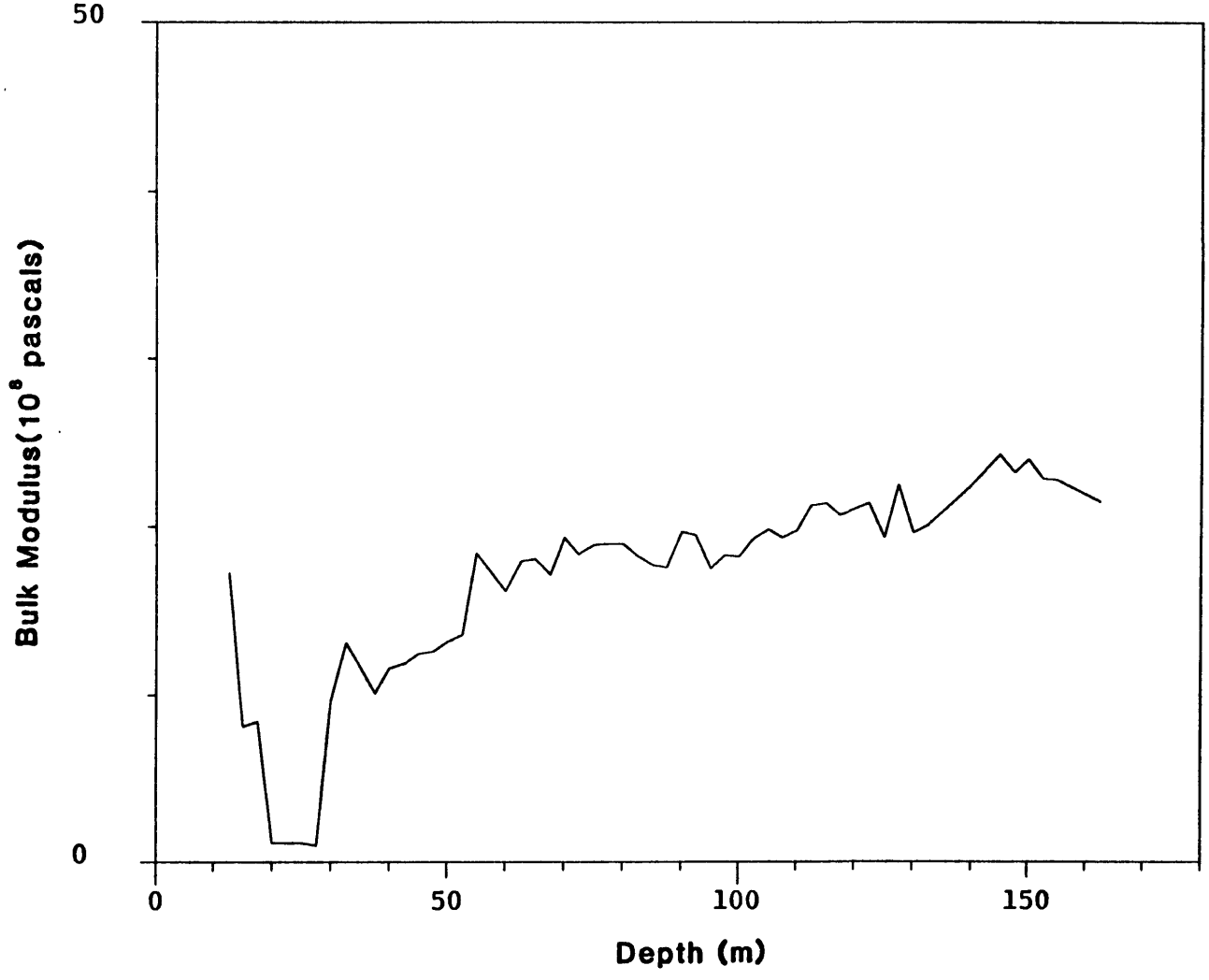

Figure 3b

Plot of K (10^8 Pa.) as a function of depth (meters) for the Vinyard Canyon site.

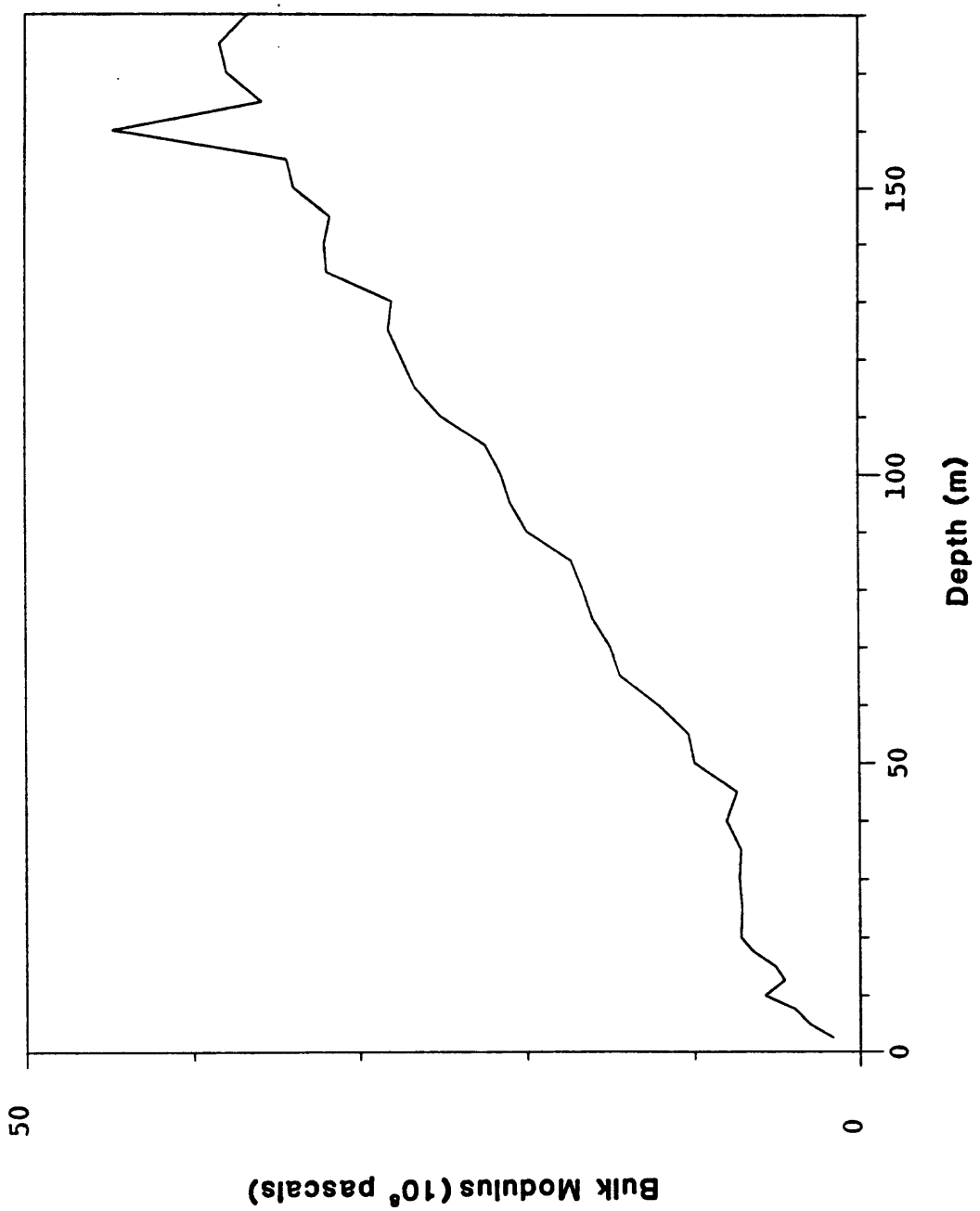

Figure 3c

Plot of K (10^8 Pa.) as a function of depth (meters) for the Red Hills site.

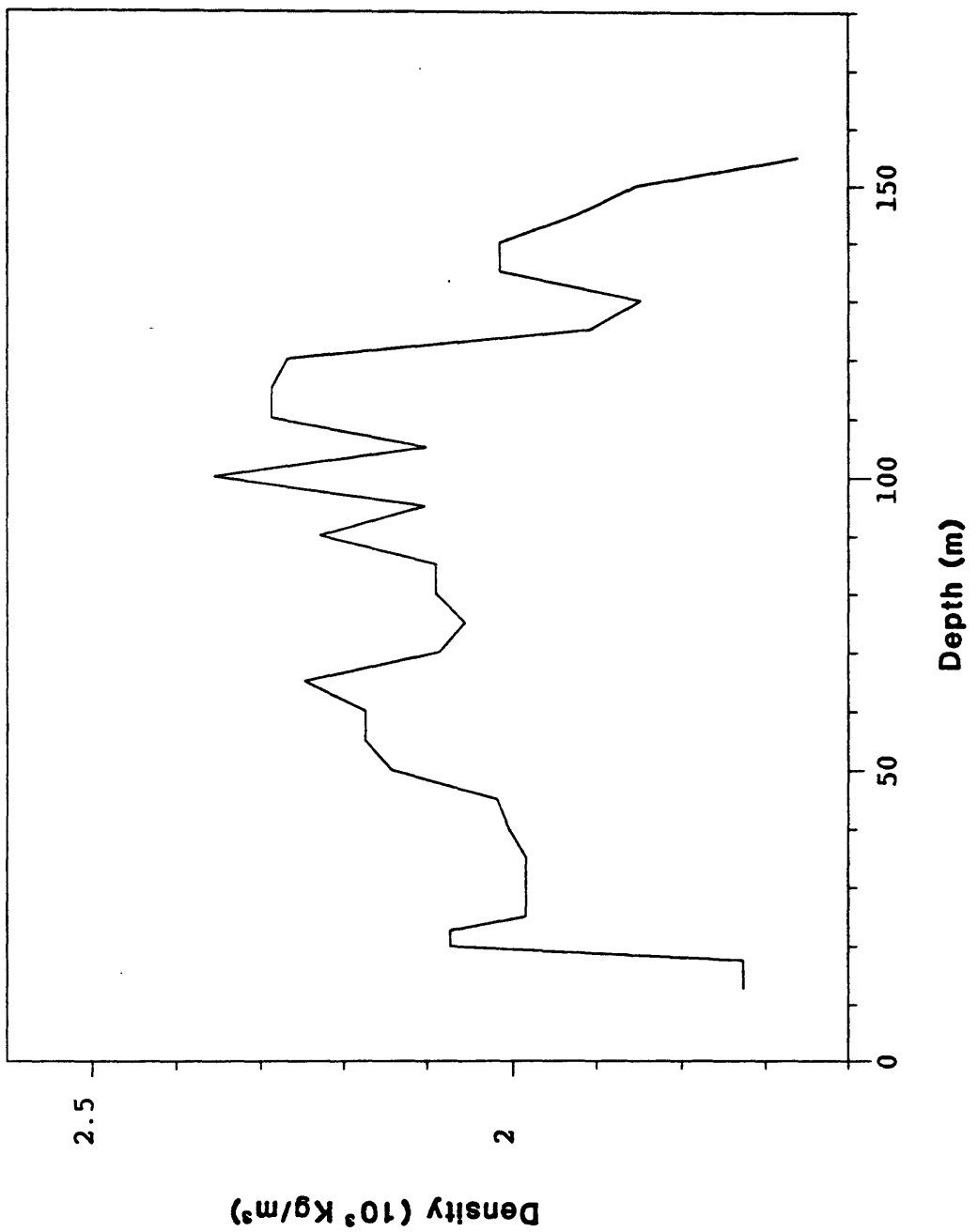

Figure 4a

Plot of ρ (10^3 Kg/M^3) as a function of depth (meters) for the Stockdale Mountain site.

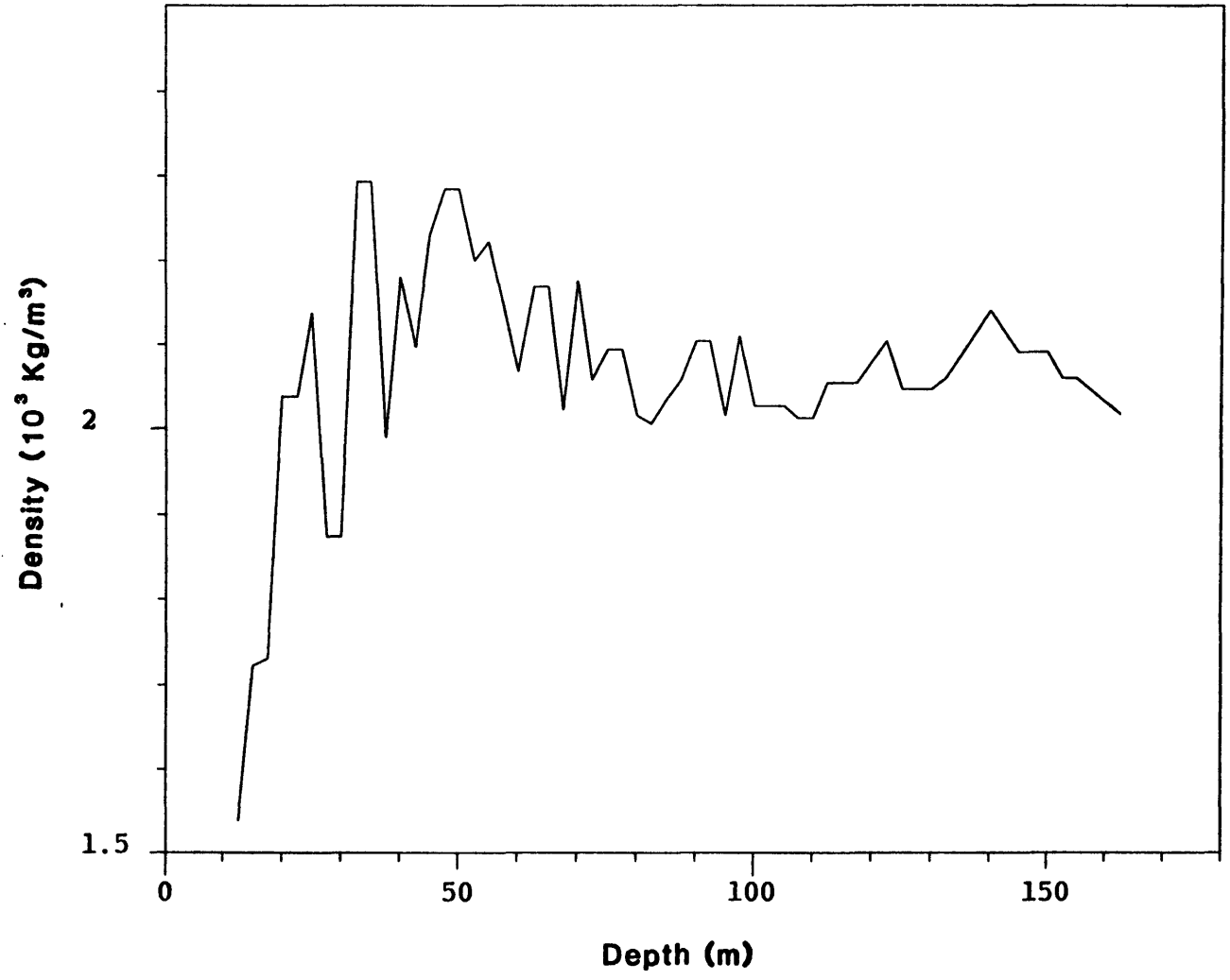

Figure 4b

Plot of ρ (10^3 Kg/M^3) as a function of depth (meters) for the Vineyard Canyon site.

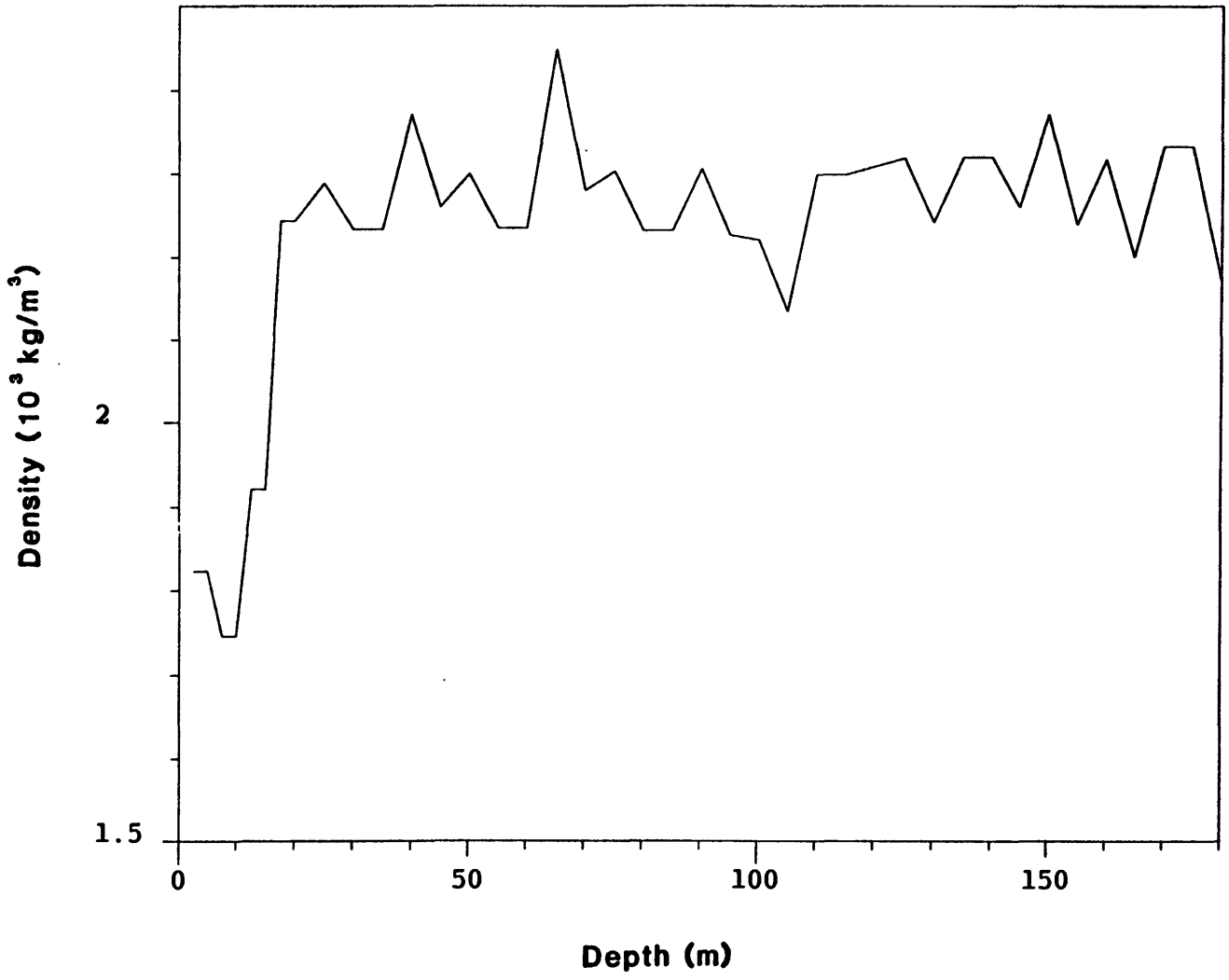

Figure 4c

Plot of ρ (10^3 Kg/M^3) as a function of depth (meters) for the Red Hills site.

the system would be similar to that expected for "blocklike" fault interaction such as was suggested by Hill (1982), and Weldon and Humphreys (1986) to describe many of the geometric features of the San Andreas fault system.

A second possibility is that the low values result from the weaker near-surface materials. Measurements of seismic velocity in other boreholes (Fletcher et al., 1990) in sites not adjacent to a major fault system indicates: 1) that within 30 m of the surface the seismic velocities are four or five times greater than those observed here, and 2) the effects of very near-surface materials fall of very quickly with depth. It seems more likely that the effects we observe result from a weak vertical fault system rather than the effects of near-surface weak layering.

Models of weak vertical fault systems have been developed by Kasahara and Rybicki (1977), McHugh and Johnston (1977), Mahrer (1986), and others. The difficulty with these models was the absence of constraints on μ and K. The values observed here indicate that the shear modulus, or rigidity, may be as much as 10 times lower in the near-fault regime than in more competent rocks found at greater distances from an active fault system. The implications of this are that strain accumulation and release will be correspondingly higher within the fault zone materials. This may explain some of the observations in China of precursory strain changes near faults sometimes at great distances from the subsequent earthquake.

ACKNOWLEDGEMENTS

We would like to thank Tom Moses of the U.S. Geological Survey for the use of his lab, and his helpful advise.

REFERENCES

Bakun, W.H. and Lindh, A.G., (1985). The Parkfield, California Earthquake Prediction Experiment, *Science,* **229**, 619-624.

Birch, F., (1966). Compressibility; Elastic Constants, *Handbook of Physical Constants,* Sydney P. Clark, editor, 97-173.

Fletcher, J., Gibbs, J.F. and Roth, E.F., (1990). Seismic Velocities and Attenuation from Borehole measurements near Anza California, *Bull. Seis. Soc. Am.,* **80**, 807-831.

Gibbs, J.F. and Roth, E.F., (1989). Seismic Velocities and Attenuation from Borehole measurements near The Parkfield Prediction Zone, Central California, *Earthquake Spectra,* **5**, 513-537.

Gibbs, J.F., Roth, E.F., Fumal, T.E., Jasek, N.A., and Emslie, M.A., (1990). Seismic Velocities From Borehole Measurements at Four Locations along a Fifty-kilometer Section of the San Andreas Fault near Parkfield, California, *U.S. Geological Survey Open-File Report,* **90**-248.

Hill, D.P. (1982) Contemporary Block Tectonics: California and Nevada, *Journal of Geophysical Research,* **87**, 5433-5450.

Johnston, M. J. S., R. D. Borcherdt, M. T. Gladwin, G. Glassmoyer, and A. T. Linde (1987). Fault failure with moderate earthquakes, *Tectonophys.,* **144**, 189-206.

Mahrer, K., (1981). Strike-Slip Faulting in a Bi-Directionally Varying Crust, *Bull. Seis. Soc. Am.,* **71**, 391-404.

McHugh, S. and Johnston, M., (1977). Surface Shear, Stress, and Shear Displacement for Screw Dislocations in a Vertical Slab with Shear Modulus Contrast, *J.*

Geophys. Res., **49**, 715-722.

Myren, G.D. and Johnston, M.J.S., (1989). Borehole Dilatometer installation, Operation and Maintenance at Sites along the San Andreas Fault, California, *U.S. Geological Survey, Open-File Report,* **89**-349.

Kasahara, K. and Rybicki, K., A Strike-Slip Fault in a Laterally Inhomogeneous Medium, *Tectonophysics,* **42**,127-138, 1977.

Sims, J.D., Geologic Map of the San Andreas Fault Zone in the Cholame Valley and Cholame Hills Quadrangles, San Luis Obispo and Monterey Counties, California, *U.S. Geological Survey, Map* MF-1995, 1988.

Sims, J.D., Chronology of Displacement on the San Andreas Fault in Central California: Evidence from Reversed Positions of Exotic Rock Bodies Near Parkfield, California, *U.S. Geological Survey, Open-File Report,* **89**-571, 1989.

Stacey, F.D., *Physics of the Earth,* John Wiley and Sons New York, NY, 1969.

Weldon, R. and Humphreys E., A Kinematic Model of Southern California, *Tectonics,* **5**,33-48, 1986.